J. Braz. Chem. Soc., Vol. 21, No. 7, 1366-1376, 2010.
Printed in Brazil - ©2010 Sociedade Brasileira de Química
0103 - 5053 $6.00+0.00

Article

Chemical Modification of Niobium Layered Oxide by Tetraalkylammonium Intercalation

Ana L. Shiguihara,[a] Marcos A. Bizeto[b] and Vera R. L. Constantino*[,a]

[a]Instituto de Química, Universidade de São Paulo, Av. Prof. Lineu Prestes 748, 05508-000 São Paulo-SP, Brazil

[b]Departamento de Ciências Exatas e da Terra, Universidade Federal de São Paulo - Campus Diadema, Rua Prof. Artur Riedel 275, 09972-270 Diadema-SP, Brazil

A modificação química do material lamelar $K_4Nb_6O_{17}$ foi investigada sistematicamente através da reação de sua forma protônica ($H_2K_2Nb_6O_{17}$) em soluções alcalinas contendo os cátions tetrametilamônio (tma^+), tetraetilamônio (tea^+) ou tetrapropilamônio (tpa^+). A quantidade intercalada corresponde a 50% (para tma^+), 25% (para tea^+) e 15% (para tpa^+) da carga negativa do $H_2K_2Nb_6O_{17}$ (considerando a troca iônica na região interlamelar I). As amostras de hexaniobato apresentam reflexões basais (020) de 23,0, 26,3 e 26,5 Å quando intercaladas, respectivamente, com tma^+, tea^+ e tpa^+. Aquecendo-se as amostras acima de 200-250 °C, observa-se a liberação de CO_2; a reação de eliminação de Hofmann também é observada para as amostras de hexaniobato-tpa^+. As imagens de microscopia eletrônica de varredura mostram a presença predominante de partículas em forma de placas; partículas em forma de bastões também são observadas nas amostras contendo íons volumosos. A reação de intercalação é promovida na ordem $tma^+ > tea^+ > tpa^+$, enquanto a formação de uma dispersão de partículas coloidais é facilitada na ordem inversa.

Chemical modification of the layered $K_4Nb_6O_{17}$ material was systematically investigated through the reaction of its proton-exchanged form ($H_2K_2Nb_6O_{17}$) in alkaline solutions containing tetramethylammonium (tma^+), tetraethylammonium (tea^+) or tetrapropylammonium (tpa^+) cations. The intercalated amount reaches 50% (for tma^+), 25% (for tea^+) and 15% (for tpa^+) of the $H_2K_2Nb_6O_{17}$ negative charge (concerning the exchange at interlayer I) due to the steric hindrance of larger cations. Hexaniobate samples present (020) basal reflections equal to 23.0, 26.3 and 26.5 Å once intercalated respectively with tma^+, tea^+ and tpa^+. When samples are heated above 200-250 °C, CO_2 evolution is observed; Hofmann elimination reaction is also detected for hexaniobate-tpa^+ samples. Scanning electron microscopy images show the predominance of plate-like particles; stick-like particles are also observed for samples containing bulky ions. The intercalation reaction is promoted in the order $tma^+ > tea^+ > tpa^+$, while the formation of a dispersion of colloidal particles is facilitated in the inverse order.

Keywords: layered niobate, hexaniobate, tetraalkylammonium, intercalation

Introduction

New materials have been prepared combining chemical species that show unlike properties such as organic, inorganic and biochemicals in order to develop systems with improved or unique performance. However, the design of these hybrid materials requires chemical strategies to compatibilize so dissimilar species at the nanoscopic domain. One plausible approach demands the use of chemical reactions or processes that enhance the physicochemical interactions among the counterparts.

Considering inorganic phases, suitable reactions to increase the interaction with organic species consist in *(i)* functionalization of the inorganic surfaces through covalent bonds with appropriated pendent groups or *(ii)* ion exchange of charged species that neutralize inorganic surfaces by proper ions.[1] Chemical modification of inorganic nanostructures or nanocrystals has deserved special attention in the recent literature.[1,2] Organic-inorganic and biochemical-inorganic hybrid materials can be explored in diversified studies concerning the

*e-mail: vrlconst@iq.usp.br

preparation of nanostructured thin-films, macro- or mesoporous solids, biomaterials, biosensors, polymer nanocomposites, catalysts and photocatalysts, devices for generation of photocurrent or photoluminescence, and hierarchical structures.[1,2]

Among the inorganic materials, the layered frameworks can produce nanostructured hybrid materials by intercalation of guest species between the layers or reassemblage of the anisotropic nanosheets produced in an exfoliation process. Layered niobates are an important class of inorganic materials that have some interesting characteristics such as semiconducting property, photosensitivity, acidic sites, high aspect ratios, chemical stability in a large range of pH and high loading capability. They are constituted of negative layers of NbO_6 octahedral units (linked by corner and/or edge) and potassium cations between adjacent layers.[3]

Chemical modification of the niobate interlayer region and surface properties based on functionalization reactions can be achieved using the proton exchanged phases. Organic groups covalently bonded to the interlayer and external surfaces of niobate materials were obtained by reaction between the acidic Nb-OH group and *n*-alcohols such as methanol, ethanol and others with longer alkyl chains,[4] polyethers of $CH_3(OCH_2CH_2)_mOH$ ($1 \leq m \leq 4$) composition,[5] trifluoracetate[6] and silanes forming Nb-O-Si bonds.[7]

As mentioned above, another strategy to perform the chemical modification of niobate materials comprises the intercalation of organic cations. In the pioneer work of Lagaly and Beneke,[8] interlayer simple inorganic cations were exchanged by *n*-alkylammonium (C_4-C_{18}) ions. Later on, other papers were published about the intercalation of *n*-alkylammonium[9] and also of substituted alkylammonium ions (hydroxyl and diamines)[10] into layered niobate materials.

One important motivation for the replacement of simple cations such as potassium by organic ions is to overcome the high layer charge density of niobates that precludes the intercalation of bulky species. As the organic modified derivatives are more reactive than the pristine solids, they are used as a pre-intercalated precursor for preparation of niobates intercalated with bulky species such as porphyrins,[11] rhodamine[12] and anthocyanines,[13] as well as for adsorption of organic compounds like phenols.[14]

Chemical modification of niobate by the intercalation route is mainly driven by the fact that the pre-intercalation with polyether monoamine surfactant,[15] tetraalkylammonium ion (from tetrabutylammonium hydroxide solutions),[16] and *n*-alkylammonium ion[17] promotes the exfoliation of layered niobate. This process produces a colloidal dispersion of inorganic nanosheets, suitable for preparation of thin films to generate photocurrent using $[Ru(bpy)_3]^{2+}$ sensitizer,[18] photoluminescence from rare earth ions,[19] molecular hydrogen from water under illumination,[20] protonic conductor,[21] Li^+ conductor,[22] interstratified materials with layered double hydroxides,[23] acid catalysts,[24] macroporous niobate,[25] biosensors based on hemoglobin[26] and other materials, as reviewed recently.[27]

In addition, niobate nanosheets in colloidal dispersion can undergo a curling process forming tubular or scrolled inorganic nanoparticles under soft chemical conditions.[28] Niobate particles with such morphology can form porous inorganic-inorganic composites with aluminosilicate[29] or can incorporate cationic porphyrin[30] and complexes that are mimics of copper oxidases.[31] Nanoscrolls having $[Ru(bpy)_3]^{2+}$ as the sensitizer and edta as the sacrificial electron donor can produce molecular hydrogen from water splitting with visible light.[32]

In the present work, we conducted the chemical modification of the layered niobate of $K_4Nb_6O_{17}$ composition through reaction of its proton-exchanged form in tetraalkylammonium hydroxide solutions. Single crystal X-ray diffractometry studies of hexaniobate phases ($M_4Nb_6O_{17}$, where $M = K^+$, Rb^+ or Cs^+) indicate that the unit cells are composed of four stacked layers along the *b*-axis direction and each layer is constituted of double NbO_6 chains in which one octahedron out of two is periodically missing in the second chain.[33] The unit cell of anhydrous $K_4Nb_6O_{17}$ is orthorhombic (a = 7.83Å, b = 33.21 Å, c = 6.46 Å) and the stacked negative layers yield two distinct interlayer regions, usually designated I and II, as seen in Figure 1. The regions are crystallographically distinct and also display unusual intercalation properties (perhaps due to the fact that only interlayer region I can be hydrated,[33] which is important for occurrence of exchange). Depending on the cation electrical charge and the experimental conditions, ion-exchange reactions take place only at interlayer I.[34,35] As a result of this peculiar feature, the cation-exchanged product has a layered structure with a second staging arrangement. Due to the high crystallinity of layered hexaniobate, this phenomenon can be experimentally detected using X-ray diffractometry[34,36] or by the indirect determination of exfoliated particles thickness.[13,16,17,28] $K_4Nb_6O_{17}\cdot 3H_2O$ structural data from atomic force microscopy (AFM) have shown a preferential surface cleavage at the water-containing interlayer I; cleavage at interlayer II is unlikely.[37] According to that, hydrogen bonds established by water molecules in interlayer I are weaker than the ionic bonds between the K^+ ion and oxygen atoms in interlayer II (Figure 1).

Potassium hexaniobate material can be changed to the protonic form when suspended in acid aqueous

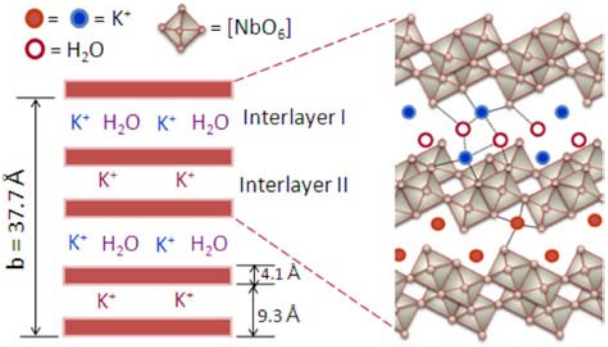

Figure 1. Representation of the $K_4Nb_6O_{17}·3H_2O$ structure. In the right hand side, solid and dashed lines among the interlayer species and the NbO_6 units represent the ionic interactions and hydrogen bonds.

solution. Under mild conditions, K^+ ion exchange is partial ($H_xK_{4-x}Nb_6O_{17}$);[16,36] considering the chemical properties of interlayers I and II mentioned above, it is usually proposed that H^+/H_3O^+ ions are present at interlayer I. The segregation of proton ions has been validated through experiments where the protonic hexaniobate is used as precursor to obtain the exfoliated material. Characterization of exfoliated particles by AFM[17,18,28] permits to estimate the particles thickness and distinguish particles constituted by two layers containing sandwiched K^+ ions. Using high resolution electron microscopy (HRTEM) images of restacked hexaniobate obtained from a dispersion of exfoliated particles, we observed bright lines related to organic species intercalated in region I and dark lines about 14 Å thick.[13] This value is very close to that obtained by the sum of two hexaniobate layers thickness and the interlayer II occupied by K^+ ions (4.1 Å plus 9.3 Å; see Figure 1). This result corroborates the proposal of the partial exchange of H^+/H_3O^+ ions only into interlayer I and the posterior exfoliation producing bilayers of $[K_2Nb_6O_{17}]^{2-}$ composition. Ellipsometric data of hexaniobate films prepared by layer-by-layer technique also allow inferring the thickness of exfoliated particles and support the assumption of the low reactivity of interlayer II.[16]

Studies of the reaction between the hexaniobate protonic form ($H_xK_{4-x}Nb_6O_{17}$) and alkylammonium hydroxide solutions are restricted to the tetrabutylammonium (tba^+) hydroxide solution.[16,24,38] $H_xK_{4-x}Nb_6O_{17}$ can react in tetraalkylammonium hydroxide solutions producing water and two kinds of materials: *(i)* intercalated materials having the alkylammonium ion between niobate layers, *(ii)* dispersions of niobate nanosheets. We have demonstrated that, in tba^+ hydroxide solutions, about 65 wt.% of the sample is delaminated and that bulky tba^+ cations are not able to intercalate in hexaniobate.[39] The material recovered from the colloidal dispersions of hexaniobate nanosheets has only 10% of H^+ ions exchanged by tba^+, since the size and charge of the organic cation preclude the balance of all niobate negative layer charge.

In this study, the investigation was extended to other tetraalkylammonium (R_4N^+, where R = methyl, ethyl, propyl) hydroxide solutions, in order to investigate the influence of the carbon chain and the R_4N^+/H^+-niobate molar ratio on the intercalation reaction into proton exchanged hexaniobate material. Solid samples were analyzed by powder X-ray diffractometry (XRD), thermogravimetric analyses coupled to mass spectrometry (TGA-MS), elemental analysis, infrared (FTIR) and FT-Raman spectroscopies and scanning electron microscopy (SEM). To our knowledge, this is the first time that a systematic study about modification of the hexaniobate structure and properties through reaction in tetraalkylammonium hydroxide solutions is performed.

Experimental

Chemicals

Nb_2O_5 was obtained from Companhia Brasileira de Metalurgia e Mineração (CBMM, Brazil) and K_2CO_3 was supplied by Merck. Aqueous solutions containing 25% tetramethylammonium (tma^+) hydroxide and 25% tetraethylammonium (tea^+) hydroxide were obtained from Acros Organics, while the 1 mol L^{-1} solution of tetrapropylammonium (tpa^+) hydroxide was obtained from Aldrich. All reagents were used as received.

Preparation of $H_2K_2Nb_6O_{17}$

$K_4Nb_6O_{17}$ was prepared by heating a stoichiometric mixture of Nb_2O_5 and K_2CO_3 at 1100 °C for 10 h (ceramic method), as previously described.[11] The isolation of the orthorhombic hexaniobate crystal structure with d_{040} = 9.4 Å was confirmed by XRD. The H^+-exchanged form was prepared by refluxing a suspension of $K_4Nb_6O_{17}$ in HNO_3 6 mol L^{-1} for 3 days. Afterwards, the isolated material was characterized by XRD and thermogravimetric analyses (TGA) as previously reported.[36] These data confirmed the isolation of the acidic hexaniobate of composition $H_2K_2Nb_6O_{17}·H_2O$ with d_{040} = 8.0 Å.

Preparation of hexaniobate-R_4N^+ (R=methyl, ethyl, propyl) samples

Tetraalkylammonium (R_4N^+) hydroxide solutions containing molar ratios R_4N^+/H^+-niobate (where H^+-niobate represents the total amount of H^+ ion in $H_2K_2Nb_6O_{17}$) of 0.25, 0.50, 0.75 and 1.0 were mixed with 0.50 g of

$H_2K_2Nb_6O_{17}$ and the final volume of the suspensions was adjusted to 250 mL, as reported in a previous study.[39] Capped flasks containing fixed amounts of $H_2K_2Nb_6O_{17}$ in $(R_4N)OH$ aqueous solution were maintained under stirring at room temperature for two weeks. The shaker was switched off overnight. After that, the flasks were kept without stirring for one day, and the opaque supernatants were separated from the deposited solids (*i.e.*, the sediment at the bottom of the flasks) using a Pasteur pipette. Afterwards, the deposited solid fractions were washed with water and dried under vacuum in a desiccator with silica gel. These solid samples are here abbreviated as R_4N(XX)dep, where XX is the R_4N^+/H^+-niobate ratio used in the experiment and "dep" means "deposited". In other words, regarding the general formula $(R_4N^+)_xH_{2-x}K_2Nb_6O_{17}$, the value of x is ranging from 0.5 (when $R_4N^+/H^+ = 0.25$) to 2.0 (when $R_4N^+/H^+ = 1$).

In order to estimate the percentage of niobate in the deposited solid, the mass of the solid that remained at the bottom of the flasks (subtracted the organic content) was compared to the mass of $H_2K_2Nb_6O_{17}$ used in the experiment (0.50 g).

Characterization methods

Elemental analysis (C, H, N) were conducted on a Perkin Elmer 2400 analyzer at the Instituto de Química (Universidade de São Paulo - USP). XRD patterns of powdered samples were recorded on a Rigaku diffractometer model Miniflex using Cu-K_α radiation (1.541 Å, 30 kV and 15 mA). Mass spectrometry-coupled thermogravimetric analyses (TGA-MS) were recorded on a Netzsch thermoanalyser model STA 490 PC Luxx coupled to an Aëolos 403C mass-spectrometer, under synthetic air (50 mL min^{-1}) at 10 $^oC\ min^{-1}$. Fourier transform infrared spectra (FTIR) were recorded on a Bomem spectrophotometer, model MB-102, with a reflectance accessory; the samples were diluted in solid KBr. Fourier-transform Raman (FT-Raman) spectra were recorded in a FT-Raman Bruker FRS-100/S spectrometer using 1064 nm exciting radiation (Nd:YAG laser Coherent Compass 1064-500N) and a Ge detector. Scanning electron micrographs of gold-coated samples were recorded on a Leo 440i microscope with a SiLi detector (secondary electrons) at the Instituto de Geociências (Universidade de São Paulo - USP).

Results and Discussion

Carbon, nitrogen, hydrogen and water contents of all samples isolated from the $H_2K_2Nb_6O_{17}$ suspension in tetraalkylammonium hydroxide solution, as well as the proposed chemical formulas, are reported in the Supplementary Information (SI, Tables S1-S3). Figure 2 shows the relation between the nominal and experimental value of x regarding the general formula $(R_4N^+)_xH_{2-x}K_2Nb_6O_{17}$. It was noticed that, for tma^+, tea^+ and tpa^+ ions, intercalation between the hexaniobate layers occurred, but only a limited amount of the organic cation can replace the H^+/H_3O^+ ions. Besides, the amount of the layers negative charge neutralized by the organic ions decreases with the increasing carbon chain length of the tetraalkylammonium cation, almost certainly due to the superior steric hindrance of larger ions. The content of organic ammonium ions increases with the rise in the R_4N^+/H^+ molar ratio, and the intercalated amount reaches 50% ($R_4N^+ = tma^+$), 25% ($R_4N^+ = tea^+$) and 15% ($R_4N^+ = tpa^+$) of the negative charge of $H_2K_2Nb_6O_{17}$, concerning the exchange reaction only at the interlayer space I.

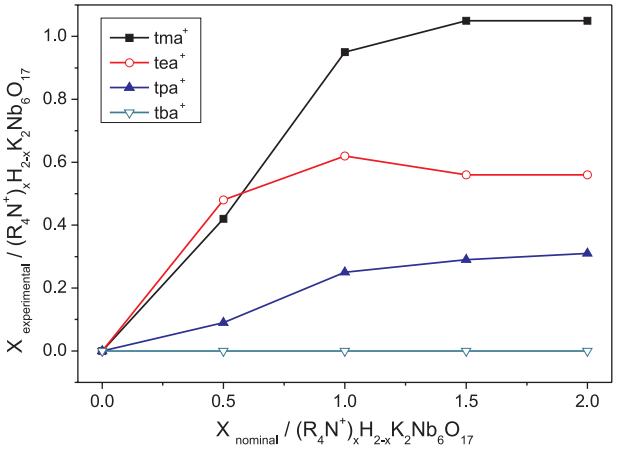

Figure 2. Experimental *versus* nominal values of X in the general formula $(R_4N^+)_xH_{2-x}K_2Nb_6O_{17}$, where R_4N^+ = tetraalkylammonium cation.

X-ray diffraction patterns of the protonic niobate and the R_4N^+-intercalated niobates are shown in Figure 3. The XRD pattern of $H_2K_2Nb_6O_{17}$ shows a basal spacing (d_{040}) of 8.0 Å and the absence of the 020 diffraction peak, as expected.[30,36,39,40] The calculated d_{040} value is consistent with the intercalation of one water molecule in the protonic phase.[8] After the intercalation of R_4N^+ cations, the peak attributed to the 020 interplanar distance appears, as well as the second, third and fourth order reflections. The exception is observed with tba^+, for which the diffraction pattern indicates that this cation does not intercalate into the hexaniobate. The shifts in the diffraction peaks of the niobate treated with tba^+, as compared to the $H_2K_2Nb_6O_{17}$ diffraction peaks, are not related to the alkylammonium intercalation; the corresponding increase in the basal spaces is too small for tba^+ cation intercalation. The peak shifts can be attributed to the presence of $H_2K_2Nb_6O_{17}$

phases containing different amounts of interlayered water molecules.[39] Abe *et al*.[40] also observed a proton-exchanged phase having a 040 basal spacing of about 9 Å.

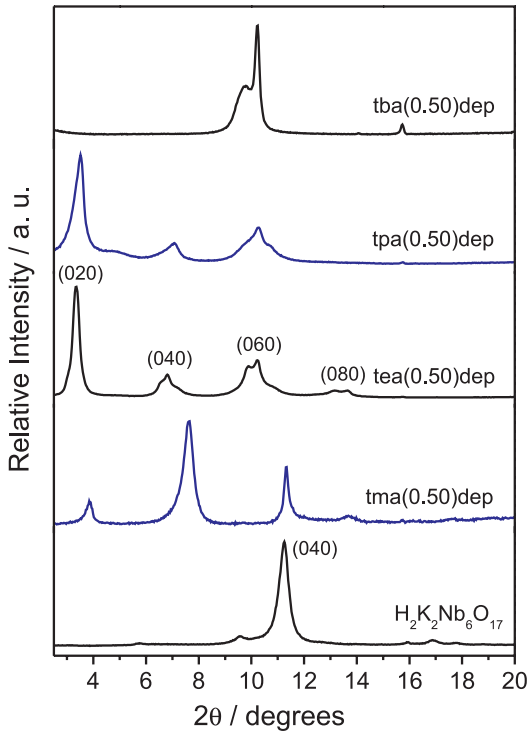

Figure 3. XRD patterns of $H_2K_2Nb_6O_{17}$, tma(0.50)dep, tea(0.50)dep, tpa(0.50)dep and tba(0.50)dep.

Isolated hexaniobate-tma$^+$ samples present basal reflections (0k0) equal to 23.0 Å (020), 11.5 Å (040) and 7.79 Å (060), while hexaniobate-tea$^+$ solids show basal spacings of 26.3 Å (020), 13.0 Å (040), 8.64 Å (060) and 6.48 Å (080). For the hexaniobate-tpa$^+$ samples, basal reflections are 26.5 Å (020), 13.1 Å (040) and 8.64 Å (060). Considering the 0k0 reflections where k = 2, 4, 6, the mean values of the b_o unit cell parameters are 46.4 Å, 52.0 Å and 52.4 Å for the systems intercalated respectively with tma$^+$, tea$^+$ and tpa$^+$. Based on the chemical properties of hexaniobate interlayers I and II, and also the fact that the precursor $H_2K_2Nb_6O_{17}$ has the H^+/H_3O^+ ions located in interlayer I, we propose that the organic cations are preferentially intercalated in region I, as illustrated in Figure 4. Hence, proton-exchanged hexaniobate mixed with hydroxide solutions of small tetraalkylammonium cations generate mainly intercalated materials (reaction A in Figure 4), while bulky ions such as tba$^+$ favor the formation of niobate nanosheets (reaction B in Figure 4).

The intercalation of R_4N^+ ions only at interlayer I was evidenced in a previous study,[13] in which the tea(0.50) sample was used as a precursor to intercalate flavylium cations (anthocyanins) between hexaniobate layers. The

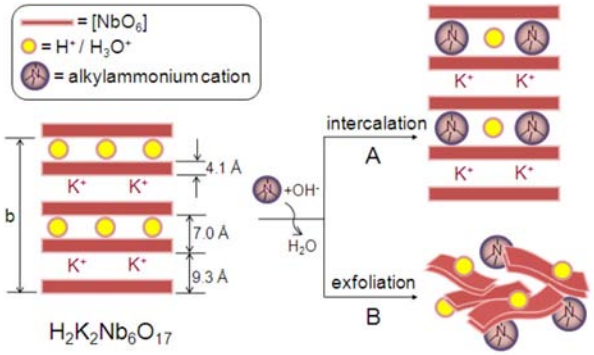

Figure 4. Schematic representation of the acid-base reaction between the hexaniobate acidic form and tetraalkylammonium hydroxide solutions.

HRTEM image showed that the dark line thickness is compatible with $[K_2Nb_6O_{17}]^{2-}$ layers.

The height of adjacent layers containing confined R_4N^+ cations can be determined by subtracting the values of the hexaniobate layer thickness (4.1 Å) and the basal spacing of a potassium filled interlayer (9.3 Å) from the calculated b_o unit cell parameter, as indicated in Figure 4. Thus the estimated gallery heights are 9.6 Å for tma$^+$, 12.6 Å for tea$^+$ and 12.8 Å for tpa$^+$. These values could be compared to the radius of the organic cations in order to analyze the arrangement of the ions between the layers. However, there is a divergence of about 30 to 50% in the reported values estimated on various scales for R_4N^+ radii.[41] In addition, hydrated radius should be assumed in the case of these cations, since TGA and elemental analysis data confirm the hydrated nature of the hexaniobate isolated samples (Table 1). Water molecular dynamics simulation of tma$^+$ and tea$^+$ solutions having chloride or bromide ions suggests that the distance between the nitrogen atom of the cation and the oxygen atom of the water in the first shell is about 4.5-5 Å and also that water (as well as the anion) prefers the space between the alkyl groups.[42] The hydration of tetraalkylammonium ions is affected by the counterion, which in this work is the hexaniobate layer (a macroanion). Therefore, the gallery heights calculated from XRD data are in agreement with the above mentioned works.

By analyzing the basal spacing observed for the three organic cations (Figure 3), it becomes apparent that the carbon chains in the tpa$^+$ ions are bent inside the interlayer region, since it is expected a radius bigger than that of tea$^+$ ions. The energy required to convert a *trans-trans·trans-trans* (tt·tt) conformer into a *trans-gauche·trans-gauche* (tg·tg) conformer is low (about 1 kcal mol^{-1}).[43] Raman spectroscopy has been used to monitor (tt·tt) and (tg·tg) conformers of the tea$^+$ ion through the spectral changes in the $-CH_3$ rocking mode at 860-880 cm^{-1}. In the case of hexaniobate-tetraalkylammonium samples, it is not possible to perform the Raman spectral analysis of the

Table 1. TGA-MS analysis under air: weight losses (wt.%) and identification of main released species

	event 1 endo	event 2 endo	event 3 exo	event 4 exo
$H_2K_2Nb_6O_{17}$	23-117 °C Δm = 1.40% *m/z* = 18 (H_2O)	117-242 °C Δm = 1.69% *m/z* = 18 (H_2O)	242-500 °C Δm = 1.90% *m/z* = 18 (H_2O)	
tma(0.50)dep	23-140 °C Δm = 3.20% *m/z* = 18 (H_2O)	140-250 °C Δm = 2.00% *m/z* = 18 (H_2O)	250-450 °C Δm = 4.58% *m/z* = 18 (H_2O) *m/z* = 44 (CO_2)	450-850 °C Δm = 3.83% *m/z* = 18 (H_2O) *m/z* = 44 (CO_2)
tea(0.50)dep	23-135 °C Δm = 2.82% *m/z* = 18 (H_2O)	135-200 °C Δm = 1.17% *m/z* = 18 (H_2O)	200-457 °C Δm = 5.71% *m/z* = 18 (H_2O) *m/z* = 44 (CO_2)	457-800 °C Δm = 3.60% *m/z* = 18 (H_2O) *m/z* = 44 (CO_2)
tpa(0.50)dep	23-150 °C Δm = 2.50% *m/z* = 18 (H_2O)	150-215 °C Δm = 0.48% *m/z* = 18 (H_2O)	215-450 °C Δm = 3.90% *m/z* = 18 (H_2O) *m/z* = 41 (propylene) *m/z* = 43 ($CH_3CH_2CH_2$) *m/z* = 44 (CO_2)	450-800 °C Δm = 1.30% *m/z* = 18 (H_2O) *m/z* = 44 (CO_2)

conformers because their bands are superimposed with the strong niobate layers bands, as shown further on. The broadening observed in the XRD pattern of tea^+ and tpa^+-intercalated niobates might be related to phases with different water contents and not to phases with different R_4N^+ content or arrangement inside the interlayer region, since the saturation of tetraalkylammonium cations inside the layers does not depend on the charge balance alone.

It should be possible to estimate the amount of cation required to neutralize the negative charge of hexaniobate if the R_4N^+ radius (or its cross sectional area) was known. However, as discussed above, the cation radius depends on its hydration degree and also on the conformer stabilized into the layered material. The negative charge density of the niobate layer is 12.6 $Å^2$/charge, and any R_4N^+ radius value already reported gives an area larger than that occupied by one hexaniobate negative charge. Thus, the steric hindrance precludes the neutralization of the whole charge of the inorganic structure by tetraalkylammonium cations supporting only one positive charge.

FTIR spectra of the deposited solids show absorptions bands of water, ammonium ions and niobate group (Figure 5), as follows:[44,45] a strong and broad band at 3300 cm^{-1} and a medium-weak band at 1650 cm^{-1} assigned to ν_{as}(O-H) and to $\delta_s(H_2O)$, respectively; bands at 1480 cm^{-1} assigned to $\delta_s(CH_2)$ of the organic cations; a strong and broad absorption band in the 900-600 cm^{-1} region related to the NbO_6 units. Bands ascribed to the organic species do not appear in the spectrum of the tba(0.50)dep sample, because the intercalation does not occur.[39] FTIR spectra of R_4N^+-hexaniobate samples present weak bands in the 3000-2800 cm^{-1} range, attributed to the asymmetrical and symmetrical stretching modes of methylene and methyl groups. The band related to the bending $\delta_s(CH_2)$ mode is sensitive to the amount of tetraalkylammonium ions in the samples, once its intensity raises in the order $tma^+ > tea^+ > tpa^+$, agreeing with elemental analyses and

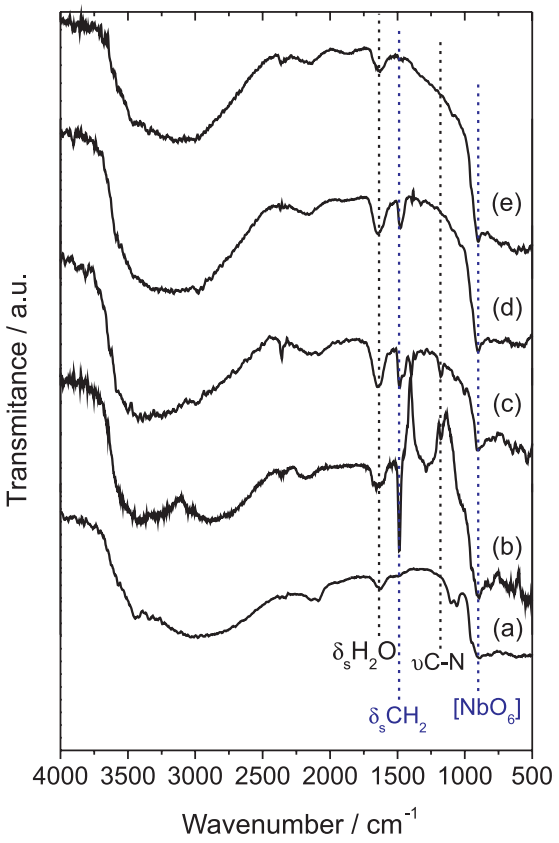

Figure 5. FTIR spectra of (a) $H_2K_2Nb_6O_{17}$, (b) tma(0.50)dep, (c) tea(0.50)dep, (d) tpa(0.50)dep and (e) tba(0.50)dep.

TGA data. The influence of R_4N^+ ions on the stretching modes of octahedral NbO_6 groups could provoke modifications in the 900-700 cm^{-1} region, but they are not perceived in the infrared spectra. As discussed ahead, Raman spectra are more responsive to the presence of organic species.

Figure 6 shows the Raman spectra of $K_4Nb_6O_{17}$, $H_2K_2Nb_6O_{17}$ and hexaniobate samples containing a low and the highest amount of intercalated tma^+ ions. In the 4000-2500 cm^{-1} region, the FTIR spectra of hexaniobate-tetraalkylammonium systems are dominated by intense and broad bands arising from water, while the Raman spectra are nearly free from such interference. Bands related to C–H stretching modes are observed at 3032, 2984, 2928 and 2822 cm^{-1} for (tma)dep samples; 2998, 2948 and 2897 cm^{-1} for (tea)dep samples; and 3004, 2973, 2938 and 2880 cm^{-1} for (tpa)dep samples. The bands at 1453 and 757 cm^{-1} are assigned to the CH_3 bending mode and the symmetric stretching vibration of the C_4N^+ group, respectively.[46]

The very intense bands in the FT-Raman spectra showed in Figure 6 are characteristic of hexaniobate as follow: 950-800 cm^{-1} (Nb–O terminal stretching mode of highly distorted NbO_6 octahedra), 700-500 cm^{-1} (Nb–O stretching of slightly distorted octahedra) and 300-200 cm^{-1} (bending modes of the Nb–O–Nb linkages).[45] The band at 900 cm^{-1} shifts to 938 cm^{-1} after the replacement of K^+ by H^+/H_3O^+ ions, as reported previously.[34,47] In the potassium form, the interlayer cations interact with the oxygen atoms of the inorganic layers and also with water molecules.[33] Replacement of K^+ by protons increases the bond order of the short and terminal Nb–O bonds because H^+ ions are probably shielded by the hydration sphere, precluding interaction with the layers.[48] As can be seen in Figure 6, the partial substitution of protons by tma^+ provokes the appearance of a new band at about 900 cm^{-1}, suggesting an increase in the Nb=O bond order. The shoulder at about 940 cm^{-1} in the spectrum of tma(1.0)dep can be attributed to the antisymmetric stretching vibration of the C_4N^+ group.[46] When the samples of hexaniobate saturated with the other tetraalkylammonium ions are considered (tea(1.0)dep and tpa(1.0)dep), the disappearance of the band at 938 cm^{-1} and the growth of a band at 900 cm^{-1} are also noticed. Hence, independently of the R_4N^+ ion intercalated, the band related to Nb=O shifts to 900 cm^{-1}. The same decrease in intensity and displacement of the band at 938 cm^{-1} is observed when $H_2K_2Nb_6O_{17}$ is dehydrated, suggesting that, after elimination of the water molecules, H^+ ions can establish a strong interaction with oxygen atoms, decreasing the Nb–O bond order.[48]

TGA and C, H, N analysis data show that the amount of water in the interlayer region decreases when R_4N^+ cations are intercalated. Hence, the presence of the organic species should promote the enhancement of the interaction between H^+ and Nb=O. The R_4N^+ cations can be localized more distant of Nb–O terminal groups situated on the layer.

TGA and DTG-MS curves (in air) of $H_2K_2Nb_6O_{17}$ and the samples saturated with tetraalkylammonium cations are showed in Figures 7 and 8 respectively. It is possible to identify four main thermal steps of weight loss, as indicated

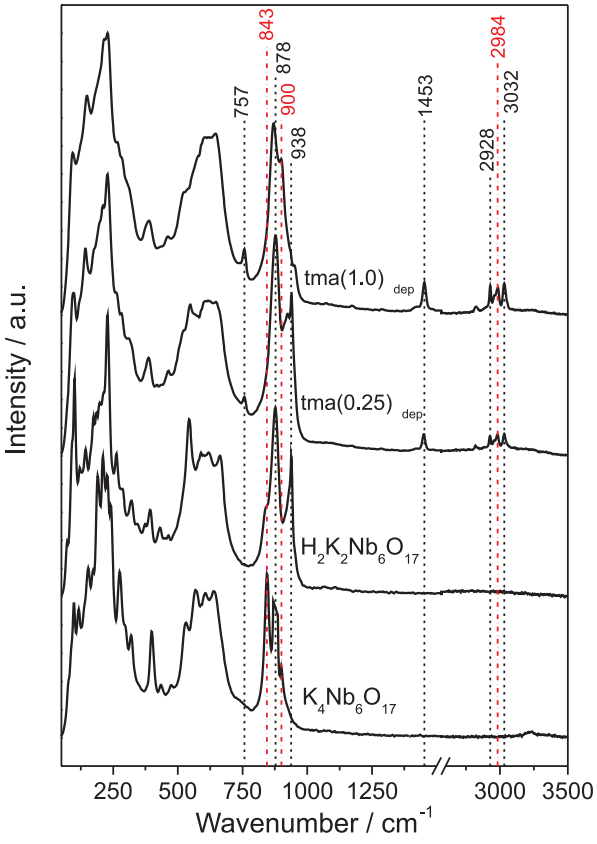

Figure 6. FT-Raman spectra of $K_4Nb_6O_{17}$, $H_2K_2Nb_6O_{17}$, tma(0.25)dep and tma(1.0)dep.

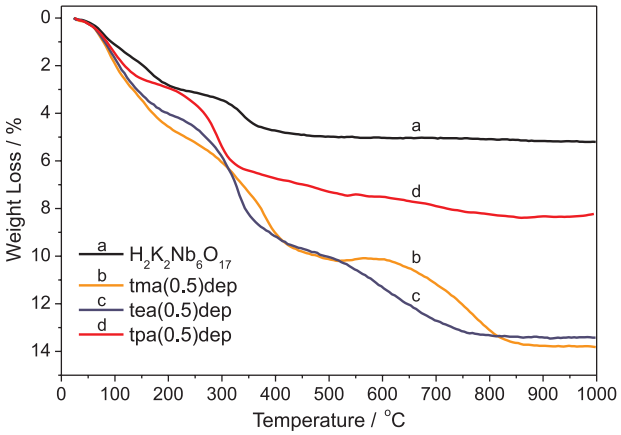

Figure 7. TGA curves of $H_2K_2Nb_6O_{17}$, tma(0.50)dep, tea(0.50)dep and tpa(0.50)dep.

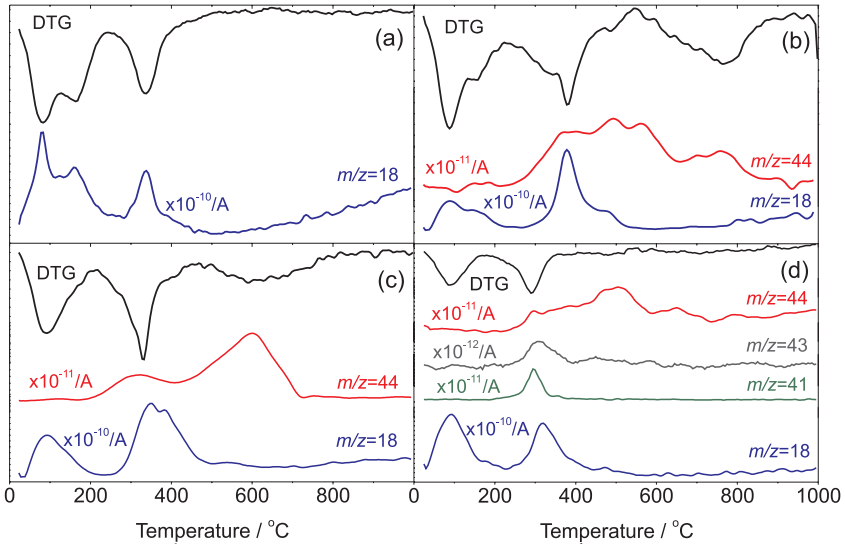

Figure 8. DTG-MS curves of (a) $H_2K_2Nb_6O_{17}$, (b) tma(0.50)dep, (c) tea(0.50)dep and (d) tpa(0.50)dep.

in Table 1. According to mass spectrometry data, the first and the second events (from room temperature to about 200-250 °C) correspond to release of the water molecules. The dehydration step at low temperature (up to about 140-150 °C) can be assigned to the interparticles water release; the dehydration process at higher temperatures (event 2) should be due to the liberation of interlayer water molecules. The water content in the hexaniobate modified by organic cation intercalation shows a tendency to decrease in the order $tma^+ > tea^+ > tpa^+$ (Table 1, event 2), which can be explained by the increase of the nonpolar surface of the tetraalkylammonium ions in the same order.[49] Above *ca*. 250°C, the $H_2K_2Nb_6O_{17}$ sample undergoes a dehydroxylation reaction (event 3) producing Nb_2O_5, $K_2Nb_4O_{11}$ and one water molecule *per* formula.[36]

For the hexaniobate samples intercalated with tetraalkylammonium cations, besides the dehydroxylation of the layers, event 3 also comprises the partial oxidation of guest ions, evidenced by the evolution of carbon dioxide. Mass spectra of gases released from hexaniobate-tpa^+ samples during the third step of weight loss also present peaks assignable to propylene (most intense characteristic fragment appears at *m/z* 41) and the propyl fragment ($CH_3CH_2CH_2$–), suggesting that a Hofmann elimination reaction also occurs:

$$(CH_3CH_2CH_2)_4N^+ \rightarrow (CH_3CH_2CH_2)_3N + H^+ + CH_3CH{=}CH_2$$

Tripropylamine molecules can be protonated when produced and kept between the layers, undergoing progressive Hofmann elimination reaction and/or oxidative degradation under air. It is noticed that, for the smallest cations, release of olefins and trialkylamine is not observed under the present experimental conditions. Hofmann elimination reaction does not occur for tma^+ but it could happen for tea^+. Also, ammonia or nitrogen oxides have not been detected for any of the samples under the experimental conditions described in this work.

SEM images of some hexaniobate-R_4N^+ deposited solids show the existence of particles with different shapes according to the amount and nature of the tetraalkylammonium cation used. In the case of hexaniobate intercalated with tma^+ and tea^+, the images of all samples show a clear predominance of plate-like particles, as expected for the non-exfoliated layered hexaniobate. However, the presence of some stick-like particles mixed with the plate-like ones is observed in the SEM images of samples containing tpa^+ (Figures 9a and 9b) and tba^+ (Figure 9c). The amount of stick-like particles increases when the R_4N^+/H^+ molar ratio used in the experiments is raised, as shown in Figures 9a and b.

For hexaniobate deposited solids obtained after contact with tba^+ solutions for two weeks, spherical particles are also observed in minor quantities. With the images registered till now it is not possible to ascertain if these specific particle shapes are constituted of a single particle or an aggregation of smaller ones. The reason for the existence of these different kinds of particle shapes (influenced by the tetraalkylammonium cation) is not yet understood and it is now under investigation in our laboratory.

The weight of the solids deposited was evaluated for the three hexaniobate-R_4N^+ systems and revealed values of about 90, 86 and 40% for tma^+, tea^+ and tpa^+ respectively. As reported previously[39] in the same experimental conditions used in this work, tba^+ ions kept 35 wt.% of particles in the deposited condition (while 65 wt.% of niobate particles

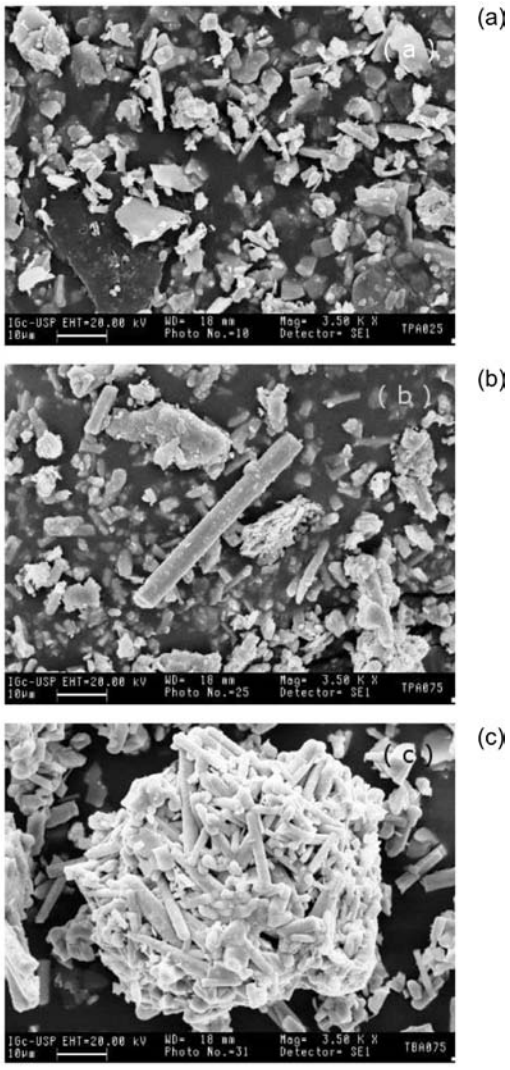

Figure 9. SEM images of (a) tpa(0.25)dep, (b) tpa(0.75)dep and (c) tba(0.75)dep.

develop a dispersion of nanosheets). Taking these results and Figure 4 into account, it is possible to claim that process A (intercalation) is promoted in the order $tma^+ > tea^+ > tpa^+$, while process B (exfoliation) is facilitated in the inverse order: $tba^+ > tpa^+ >> tea^+ > tma^+$. Tetraalkylammonium ions are symmetric species and the positive charge is located on the nitrogen atom, what means that electrostatic attraction between the organic cation and the negative charged inorganic surface decreases if the cation diameter is increased. Hence, two factors can be considered important to drive the formation of niobate nanosheets from acidic-hexaniobate in tetraalkylammonium hydroxide solutions: the R_4N^+ electrostatic attraction to the inorganic layers and the steric hindrance.

Between the extreme situations (intercalated or exfoliated samples), another process was perceived. A system with a gel-like aspect is observed when some hexaniobate-tetraalkylammonium samples are washed in order to remove the non-intercalated cations, *i.e.*, when the ionic strength decreases. The XRD pattern of a hexaniobate gel-like sample in the wet state does not show diffraction peaks (data not shown), suggesting that removing the ions by washing can lead to a long-range swelling of the layers and a disorganized arrangement of the hexaniobate sheets. The gel-like aspect was mainly observed for the hexaniobate-tea^+ samples. Bearing in mind the four tetraalkylammonium ions focused in the present work, tea^+ has an intermediate character when the ion surface polarity and the electrostatic interactions established by the R_4N^+ ions are considered.[49] While tma^+ (that shows high surface polarity) produces the most highly hydrated samples and tpa^+ (or tba^+) ions are bulky enough to promote a high delamination degree, tea^+ ions have the better hydrophilicity/size relation to form a gel-like system. It is possible to infer that the gel is not constituted by exfoliated particles but by disorganized and long-range swelled particles. The tea(0.50)dep sample in the gel-like form was used to intercalate flavylium cations (anthocyanins) and the SEM and TEM images confirmed that the hexaniobate particles were not exfoliated.[13] The particles morphology is different when compared to the images of hexaniobate-flavylium obtained from a colloidal dispersion of exfoliated nanosheets.

Conclusions

Intercalation of the tetraalkylammonium tma^+, tea^+ and tpa^+ ions in $H_2K_2Nb_6O_{17}$ is promoted by an acid-base reaction, but steric hindrance of the cations precludes the neutralization of all interlayered H^+ ions. Regarding the general formula $(R_4N^+)_xH_{2-x}K_2Nb_6O_{17}$, the X value reaches about 1.0 for tma^+ systems, 0.56 for tea^+ samples and 0.31 for tpa^+ materials. X-ray diffraction patterns indicated that the gallery height of adjacent layers containing confined R_4N^+ species is compatible with a monolayer of hydrated ions and, in the case of samples with tpa^+ ions, the carbon chain should be in a *trans-gauche* conformation. FTIR and FT-Raman spectra present bands related to water molecules, organic cations and the inorganic framework. The band assigned to the stretching of Nb=O group (pointing out to the interior of interlayer region) is shifted to low frequency due to an increase in the interaction between the niobyl group and the H^+ ions. The presence of tetraalkylammonium ions decreases the H_2O content between the layers; water molecules can shield the Nb=O···H^+ interaction.

TGA and DTG-MS curves support this interpretation, since the water content in the modified hexaniobate decreases in the order $tma^+ > tea^+ > tpa^+$, *i.e.*, when the nonpolar surface of the tetraalkylammonium ions increases.

When heated above 200-250 °C, organic ions experience an oxidative decomposition producing carbon dioxide; in the case of niobate samples containing tpa^+, a Hofmann elimination is also observed. Hexaniobate-R_4N^+ deposited solids have plate-like particles, as expected for the non-exfoliated layered hexaniobate. However, stich-like particles are also observed when $H_2K_2Nb_6O_{17}$ is kept in solutions containing the larger tpa^+ and tba^+ ions. Considering the amount of hexaniobate that is retained at the bottom of the suspensions and the amount that is delaminated (the supernatant colloidal dispersion), it is plausible to state that the intercalation reaction is promoted in the order $tma^+ > tea^+ > tpa^+$, while formation of niobate nanosheets is facilitated in the inverse order: $tba^+ > tpa^+ > tea^+ > tma^+$.

Samples containing intercalated tea^+ ions form a gel-like system when washed to remove the non-intercalated ions dissolved in water. Experimental data suggest that the gel phase is not constituted by exfoliated particles but by disorganized and long-range swelled particles. This fact was interpreted as a consequence of the intermediate characteristics (surface polarity and ion radius) of the tea^+ ions compared to the others ions investigated in this study.

Supplementary Information

Supplementary data (Tables S1-S3) are available free of charge at http://jbcs.sbq.org.br, as a pdf file.

Acknowledgments

The authors acknowledge the Brazilian agencies FAPESP and CNPq for financial support and fellowships. They also would like to thank Mr. Isaac J. Sayeg, from Instituto de Geociências (Universidade de São Paulo), for his attention and suggestions regarding the acquisition of the SEM images, the Laboratório de Espectroscopia Molecular (Universidade de São Paulo) for the Raman spectra and CBMM for the sample of Nb_2O_5.

References

1. Mammeri, F.; Le Bourhis, E.; Rozes, L.; Sanchez, C.; *J. Mater. Chem.* **2005**, *15*, 3787.
2. Han, W. S.; Lee, H. Y.; Jung, S. H.; Lee, S. J.; Jung, J. H.; *Chem. Soc. Rev.* **2009**, *38*, 1904; Xu, C.; Sun, S.; *Dalton Trans.* **2009**, 5583.
3. Raveau, B.; *Rev. Inorg. Chem.* **1987**, *9*, 38.
4. Takahashi, S.; Nakato, T.; Hayashi, S.; Sugahara, Y.; Kuroda, K.; *Inorg. Chem.* **1995**, *34*, 5065; Tahara, S.; Sugahara, Y.; *Langmuir* **2003**, *19*, 9473; Suzuki, H.; Notsu, K.; Takeda, Y.; Sugimoto, W.; Sugahara, Y.; *Chem. Mater.* **2003**, *15*, 636.
5. Takeda, Y.; Momma, T.; Osaka, T.; Kuroda, K.; Sugahara, Y.; *J. Mater. Chem.* **2008**, *18*, 3581.
6. Takeda, Y.; Suzuki, H.; Notsu, K.; Sugimoto, W.; Sugahara, Y.; *Mater. Res. Bull.* **2006**, *41*, 834.
7. Tahara, S.; Takeda, Y.; Sugahara, Y.; *Chem. Mater.* **2005**, *17*, 6198; Nakato, T.; Hashimoto, S.; *Chem. Lett.* **2007**, *36*, 1240.
8. Lagaly, G.; Beneke, K.; *J. Inorg. Nucl. Chem.* **1976**, *38*, 1513.
9. Nedjar, R.; Borel, M. M.; Raveau, B.; *Z. Anorg. Allg. Chem.* **1986**, *540*, 198; Nedjar, R.; Borel, M. M.; Raveau, B.; *J. Solid State Chem.* **1987**, *71*, 451; Jacobson, A. J.; Lewandowski, J. T.; Johnson, J. W.; *J. Less-Common Met.* **1986**, *116*, 137; Abe, R.; Ikeda, S.; Kondo, J. N.; Hara, M.; Domen, K.; *Thin Solids Films* **1999**, *343-344*, 156.
10. Yakabe, S.; Nakato, T.*; J. Mater. Sci.* **2003**, *38*, 3809.
11. Bizeto, M. A.; Faria, D. L. A.; Constantino, V. R. L.; *J. Mater. Sci.* **2002**, *37*, 265.
12. Shinozaki, R.; Nakato, T.; *Microporous Mesoporous Mater.* **2008,** *113*, 81.
13. Teixeira-Neto, A. A.; Shiguihara, A. L.; Izumi, C. M. S.; Bizeto, M. A.; Leroux, F.; Temperini, M. L. A.; Constantino, V. R. L.; *Dalton Trans.* **2009**, 4136.
14. Nakato, T.; Miyashita, H.; Yakabe, S.; *Chem. Lett.* **2003**, *32*, 72; Wei, Q.; Nakato, T.; *Microporous Mesoporous Mater.* **2006**, *96*, 84; Nakato, T.; Kameyama, M.; Wei, Q.; Haga, J.; *Microporous Mesoporous Mater.* **2008**, *110*, 223.
15. Treacy, M. M. J.; Rice, S. B.; Jacobson, A. J.; Lewandowski, J. T.; *Chem. Mater.* **1990**, *2*, 279.
16. Keller, S. W.; Kim, H-N.; Mallouk, T. E.; *J. Am. Chem. Soc.* **1994**, *116*, 8817.
17. Miyamoto, N.; Yamamoto, H.; Kaito, R.; Kuroda, K.; *Chem. Commun.* **2002**, 2378; Bizeto, M. A.; Constantino, V. R. L.; *Mater. Res. Bull.* **2004**, *39*, 1811.
18. Unal, U.; Matsumoto,Y.; Tamoto, N.; Koinuma, M.; Machida, M.; Izawa, K.; *J. Solid State Chem.* **2006**, *179*, 33.
19. Ida, S.; Unal, U.; Izawa, K.; Ogata, C.; Inoue, T.; Matsumoto, Y.; *Mol. Cryst. Liq. Cryst.* **2007**, *470*, 393.
20. Izawa, K.; Yamada, T.; Unal, U.; Ida, S.; Altuntasoglu, O.; Koinuma, M.; Matsumoto,Y.; *J. Phys. Chem. B* **2006**, *110*, 4645.
21. Kobayashi, Y.; Schottenfeld, J. A.; MacDonald, D. D.; Mallouk, T. E.; *J. Phys. Chem. C* **2007**, *111*, 3185.
22. Rezende, A. R.; Bizeto, M. A.; Constantino, V. R. L.; Huguenin, F.; *J. Phys. Chem. C* **2009**, *113*, 10868.
23. Li, L.; Ma, R.; Ebina,Y.; Fukuda, K.; Takada, K.; Sasaki, T.; *J. Am. Chem. Soc.* **2007**, *129*, 8000.
24. Takagaki, A.; Sugisawa, M.; Lu, D.; Kondo, J. N.; Hara, M.; Domen, K.; Hayashi, S.; *J. Am. Chem. Soc.* **2003**, *125*, 5479.
25. Miyamoto, N.; Kuroda, K.; *J. Colloid Interface Sci.* **2007**, *313*, 369.
26. Gao, L.; Gao, Q.; *Biosens. Bioelectron.* **2007**, *22*, 1454.
27. Bizeto, M. A.; Shiguihara, A. L.; Constantino, V. R. L.; *J. Mater. Chem.* **2009**, *19*, 2512.

28. Saupe, G. B.; Waraksa, C. C.; Kim, H. N.; Han, Y. J.; Kaschak, D. M.; Skinner, D. M; Mallouk, T. E.; *Chem. Mater.* **2000**, *12*, 1556.
29. Camerel, F.; Gabriel, J. P.; Batail, P.; *Chem. Commun.* **2002**, 1926.
30. Bizeto, M. A.; Constantino, V. R. L.; *Microporous Mesoporous Mater*. **2005**, *83*, 212.
31. Bizeto, M. A.; Alves, W. A.; Barbosa, C. A. S.; Ferreira, A. M. D. C.; Constantino, V. R. L.; *Inorg. Chem*. **2006**, *45*, 6214.
32. Maeda, K.; Eguchi, M.; Youngblood, W. J.; Mallouk, T. E.; *Chem.Mater*. **2008**, *20*, 6770.
33. Gasperin, M.; Bihan, M. T.; *J. Solid State Chem.* **1980**, *33*, 83; Gasperin, M.; Bihan, M. T.; *J. Solid State Chem*. **1982**, *43*, 346.
34. Kinomura, N.; Kumada, N.; Muto, F.; *J. Chem. Soc., Dalton Trans.* **1985**, 2349.
35. Nakato, T.; Sakamoto, D.; Kuroda, K.; Kato, C.; *Bull. Chem. Soc. Jpn*. **1992**, *65*, 322; Bizeto, M. A.; Christino, F. P.; Tavares, M. F. M.; Constantino, V. R. L.; *Quim. Nova* **2006**, 29, 1215.
36. Bizeto, M. A.; Constantino, V. R. L.; *Mater. Res. Bull*. **2004**, *39*, 1729.
37. Shindo, H.; Kaise, M.; Kondoh, H.; Nishihara, C.; Hayakawa, H.; Ono, S.; Nozoye, H.; *Langmuir* **1992**, *8*, 353.
38. Camerel, F.; Gabriel, J. C. P.; Batail, P.; Panine, P.; Davidson, P.; *Langmuir* **2003**, 19, 10028.
39. Shiguihara, A. L.; Bizeto, M. A.; Constantino, V. R. L.; *Colloid Surf. A* **2007**, 295, 123.
40. Abe, R.; Hara, M; Kondo, J. N.; Domen, K.; *Chem. Mater.* **1998**, *10*, 1647.
41. Shchipunov, Y. A.; *Adv. Colloid Interface Sci.* **1988**, *28*, 135.
42. Krienke, H.; Vlachy, V.; Ahn-Ercan, G.; Bako, I.; *J. Phys. Chem. B* **2009**, *113*, 4360.
43. Luzhkov, V. B.; Österberg, F.; Acharya, P.; Chattopadhyaya, J.; Aqvist, J.; *Phys. Chem. Chem. Phys.* **2002**, *4*, 4640.
44. Silverstein, R. M.; Bassler, G. C.; Morril, T. C.; *Identificação Espectrométrica de Compostos Orgânicos*, Guanabara Koogan: Rio de Janeiro, Brasil, 1979.
45. Jehng, J. M.; Wachs, I. E.; *Chem. Mater.* **1991**, *3*, 100.
46. Felix, D. L.; Strauss, M.; Ducati, L. C.; Pastore, H. O.; *Microporous Mesoporous Mater.* **2009**, *120*, 187; Naudin, C.; Bonhomme, F.; Bruneel, J. L.; Ducasse, L.; Grondin, J.; Lassègues, J. C.; Servant, L.; *J. Raman Spectrosc*. **2000**, *31*, 97.
47. Kudo, A.; Sakata, T.; *J. Phys. Chem.* **1996**, *100*, 17323.
48. Bizeto, M. A.; Leroux, F.; Shiguihara, A. L.; Temperini, M. L. A.; Sala, O.; Constantino, V. R. L.; *J. Phys. Chem. Solids* **2010**, *71*, 560.
49. Takekiyo, T.; Yoshimura, Y.; *J. Phys. Chem. A* **2006**, *110*, 10829.

Received: October 8, 2009
Web Release Date: May 4, 2010

FAPESP helped in meeting the publication costs of this article.

J. Braz. Chem. Soc., Vol. 21, No. 7, S1, 2010.
Printed in Brazil - ©2010 Sociedade Brasileira de Química
0103 - 5053 $6.00+0.00

Chemical Modification of Niobium Layered Oxide by Tetraalkylammonium Intercalation

Ana L. Shiguihara,[a] Marcos A. Bizeto[b] and Vera R. L. Constantino*[,a]

[a] Instituto de Química, Universidade de São Paulo, Av. Prof. Lineu Prestes 748, 05508-000 São Paulo-SP, Brazil

[b] Departamento de Ciências Exatas e da Terra, Universidade Federal de São Paulo - Campus Diadema, Rua Prof. Artur Riedel 275, 09972-270 Diadema-SP, Brazil

Table S1. Estimated composition of hexaniobate-tma$^+$ deposited solids

Sample	C (%)	H (%)	N (%)	Water (%)
tma(0.25)dep	2.05	1.16	0.60	4.40
$[(CH_3)_4N^+]_{0.42}H_{1.58}K_2Nb_6O_{17}\cdot 2.4H_2O$	(1.94)[a]	(1.10)	(0.48)	(4.44)
tma(0.50)dep	4.41	1.79	1.29	5.23
$[(CH_3)_4N^+]_{0.95}H_{1.05}K_2Nb_6O_{17}\cdot 3H_2O$	(4.43)	(1.80)	(1.15)	(5.38)
tma(0.75)dep	4.85	1.88	1.41	5.19
$[(CH_3)_4N^+]_{1.05}H_{0.95}K_2Nb_6O_{17}\cdot 3H_2O$	(4.83)	(1.93)	(1.24)	(5.33)
tma(1.0)dep	4.86	1.85	1.42	4.86
$[(CH_3)_4N^+]_{1.05}H_{0.95}K_2Nb_6O_{17}\cdot 2.8H_2O$	(4.90)	(1.90)	(1.16)	(4.91)

[a] experimental data.

Table S2. Estimated composition of hexaniobate-tea$^+$ deposited solids

Sample	C (%)	H (%)	N (%)	Water (%)
tea(0.25)dep	4.51	1.65	0.66	4.94
$[(CH_3CH_2)_4N^+]_{0.48}H_{1.52}K_2Nb_6O_{17}\cdot 2.8H_2O$	(4.69)[a]	(1.38)	(0.71)	(4.95)
tea(0.50)dep	5.63	2.02	0.82	6.3
$[(CH_3CH_2)_4N^+]_{0.62}H_{1.38}K_2Nb_6O_{17}\cdot 3.7H_2O$	(5.39)	(1.59)	(0.71)	(6.2)
tea(0.75)dep	5.18	1.85	0.75	5.55
$[(CH_3CH_2)_4N^+]_{0.56}H_{1.44}K_2Nb_6O_{17}\cdot 3.2H_2O$	(5.30)	(1.41)	(0.91)	(5.46)
tea(1.0)dep	5.18	1.85	0.75	5.54
$[(CH_3CH_2)_4N^+]_{0.56}H_{1.44}K_2Nb_6O_{17}\cdot 3.2H_2O$	(5.24)	(1.37)	(0.72)	(5.49)

[a] experimental data.

Table S3. Estimated composition of hexaniobate-tpa$^+$ deposited solids

Sample	C (%)	H (%)	N (%)	Water (%)
tpa(0.25)dep	1.36	0.80	0.13	3.00
$[(CH_3CH_2CH_2)_4N^+]_{0.09}H_{1.91}K_2Nb_6O_{17}\cdot 1.6H_2O$	(1.39)[a]	(0.56)	(0.03)	(3.27)
tpa(0.50)dep	3.66	1.21	0.36	2.92
$[(CH_3CH_2CH_2)_4N^+]_{0.25}H_{1.75}K_2Nb_6O_{17}\cdot 1.6H_2O$	(3.68)	(1.11)	(0.28)	(2.94)
tpa(0.75)dep	4.22	1.30	0.41	2.73
$[(CH_3CH_2CH_2)_4N^+]_{0.29}H_{1.71}K_2Nb_6O_{17}\cdot 1.5H_2O$	(4.28)	(1.16)	(0.40)	(2.78)
tpa(1.0)dep	4.48	1.36	0.44	2.89
$[(CH_3CH_2CH_2)_4N^+]_{0.31}H_{1.69}K_2Nb_6O_{17}\cdot 1.6H_2O$	(4.54)	(1.27)	(0.49)	(3.00)

[a] experimental data.

*e-mail: vrlconst@iq.usp.br